MATERIALS CHEMISTRY
FRONTIERS

RESEARCH ARTICLE

View Article Online
View Journal | View Issue

Cite this: *Mater. Chem. Front.*, 2019, **3**, 420

Development and reactive oxygen-species scavenging activity of a new chemical hydrogen-generating system, $CaMg_2$-hydroxypropyl cellulose-citric acid, prepared using Laves-phase $CaMg_2$ and its relationship to chemical hardness

Shigeki Kobayashi, *[a] Kazuyoshi Chiba[b] and Takashi Tomie[c]

Received 25th September 2018,
Accepted 26th December 2018

DOI: 10.1039/c8qm00488a

rsc.li/frontiers-materials

We developed a new chemical hydrogen-generating $CaMg_2$-hydroxypropyl cellulose-citric acid (CAMGCC) system from Laves-phase $CaMg_2$ by using an arc melting method. The CAMGCC generated hydrogen gas (H_2) rapidly for 2–3 min on the addition of water. Moreover, the CAMGCC system could scavenge reactive oxygen species (ROS), such as toxic hydroxyl radicals ($^{\bullet}OH$) and superoxides ($O_2^{-\bullet}$) effectively. To develop a new chemical hydrogen-generating system that generates H_2 efficiently, it is essential to calculate the quantity (ΔQ) of electron transfer from metal and alloy to H_2O by using the absolute hardness (η) and absolute electronegativity (χ) based on chemical hardness. Metals and alloys with a large amount of calculated ΔQ can be used as excellent materials to develop a chemical hydrogen-generating system. A larger ΔQ of electron transfer from the metal to H_2O results in a greater antioxidant activity of the system. The results were supported by using the calculation results for clusters of $CaMg_2$ and Mg_3, instead of crystalline $CaMg_2$ and Mg. These studies are important in the development of chemical hydrogen-generating systems and antioxidants.

Introduction

Chemical hydrogen-storage systems or hydrogen-absorbing alloys have attracted a great deal of attention as new technologies for generating molecular hydrogen (H_2). As an antioxidant, H_2 has high potential for use in the prevention and medical treatment of diseases and it is a known alternative energy source.[1–5] At the laboratory level, investigations have been conducted to determine a method for the efficient generation of H_2 under mild (*i.e.*, physiological) conditions. Magnesium (Mg) has attracted the attention of chemists from various fields for use in chemical hydrogen-storage alloys because Mg alloys exhibit an oxidation resistance and burning resistance[6] and can absorb 3–6% of their mass of H_2.[7–9] However, temperatures of 200–500 °C are required to desorb H_2 from hydrogen-storage alloys, and therefore, such hydrogen-storage alloys cannot be used to develop antioxidants or to reduce oxidative stress at the living-cell level, which is the aim of our investigation. Therefore, we have focused on developing a chemical hydrogen-generating system that operates in H_2O rather than a Mg-based hydrogen-storage alloy or system.[10] It is difficult to use a Mg/H_2O system as an antioxidant to scavenge toxic hydroxyl radicals ($^{\bullet}OH$) and as a chemical hydrogen-generating system because the production of H_2 in the reaction $Mg + 2H_2O \rightarrow Mg^{2+} + 2OH^- + H_2$ is very slow in H_2O at room temperature.

In our most recent study, we developed a powder Mg–hydroxypropyl cellulose-citric acid (MGCC) as a chemical hydrogen-generating system using powdered Mg coated with hydroxypropyl cellulose (HPC), together with citric acid.[10] The production of H_2 from MGCC in H_2O is far superior to that by Mg in H_2O because of the solid-acid effect of citric acid on the Mg surface. We proposed a mechanism for H_2 production from the MGCC system. We also explored the development of a chemical hydrogen-generating system using soft Ca, but found it difficult and inefficient. Here, we focused on the use of Laves-phase Ca–Mg ($CaMg_2$) alloys because Laves-phase alloys are a crystal family that is known to exhibit a wide variety of physical, chemical, and magnetic properties, including hydrogen absorption into these materials. It has been reported that $CaMg_2$ alloys absorb H_2 under 10 MPa of H_2 at 240 °C. However, hydrogenated $CaMg_2$ only shows the desorption of H_2 gases above 480 °C.[9] Therefore, hydrogenated $CaMg_2$ alloys are impractical for use as antioxidants to reduce the oxidative stress of living cells.

[a] *Department of Analytical Chemistry of Medicines, Showa Pharmaceutical University, 3-3165 Higashitamagawagakuen, Machida, 194-8543 Tokyo, Japan. E-mail: kobayasi@ac.shoyaku.ac.jp*
[b] *Instrument Analysis Equipment Research Center, Showa Pharmaceutical University, 3-3165 Higashitamagawagakuen, Machida, 194-8543 Tokyo, Japan*
[c] *DIAVAC Limited, 495 Owadashinden, Yachiyo, Chiba 276-0046, Japan*

We developed a new hydrogen-generating $CaMg_2$-hydroxypropyl cellulose-citric acid (CAMGCC) system by using Laves-phase $CaMg_2$ with a method similar to that described in our previous paper.[10] The CAMGCC equivalent to MGCC generated approximately three times the volume of H_2 by the addition of H_2O than that by MGCC. The antioxidant activities of CAMGCC were determined from the IC_{50} values that were obtained by a scavenging assay of superoxide anion radicals ($O_2^{-\bullet}$) and hydroxyl radicals ($^{\bullet}OH$) that were generated by the xanthine oxidase (XOD) method[11] and H_2O_2 photolysis,[12–14] respectively. The antioxidant activities of CAMGCC were stronger than those of MGCC. We found that the antioxidant potentials of CAMGCC and MGCC are correlated to the quantity (ΔQ) of electron transfer from $CaMg_2$ and Mg to H_2O by using the chemical hardness theory. The large ΔQ of electron transfer from Laves-phase AB_2 to H_2O has a strong antioxidant activity. These results were also supported by calculated data based on the chemical hardness by using the density functional theory (DFT) method with clusters of $CaMg_2$ and Mg_3.[15] We report that it is possible to develop a new chemical hydrogen-generating system by using chemical hardness.

Results and discussion

Preparation of Laves-phase $CaMg_2$ and chemical hydrogen-generating system CAMGCC

The chemical hydrogen-generating system, CAMGCC, which generated hydrogen gas (H_2) efficiently, was prepared by using Laves-phase $CaMg_2$ alloy that was prepared by the arc melting of Mg with Ca. After arc melting, the Ca–Mg alloy was made into a fine powder by crushing with a pestle in a porcelain mortar. Fig. 1A and B show the XRD bands of anhydrous citric acid (▲) and powder Mg (●). Fig. 1C shows the powder X-ray diffraction (XRD) bands of the Ca–Mg alloy that was produced by using arc melting. It is thought that a Ca–Mg alloy of uniform composition was produced because the XRD band that was derived from Mg of $2\theta = 36.5^{\circ}$ was not observed in Fig. 1C. Moreover, the bands were identified as the diffraction peaks (○) of the $CaMg_2$ alloy that was indexed to the AB_2 Laves phase by comparison with the XRD profiles of the Laves-phase $CaMg_2$.[8,9] It was suggested that the single nanoparticles of the Ca–Mg alloy that were obtained from the chamber by the arc plasma method had broad XRD bands that were not identical to the XRD bands of the Laves-phase $CaMg_2$. This means that the fine particles were mixtures that contained Laves-phase and other phase structures.

The new chemical hydrogen-generating system CAMGCC was prepared with hydroxypropyl cellulose (HPC)-coated Laves-phase $CaMg_2$ (powder) with anhydrous citric acid according to the method described in the experimental section. The XRD bands of the powder CAMGCC system were identified as the diffraction peaks of $CaMg_2$ (○) and citric acid (▲) as shown in Fig. 1D.

Generation of H_2 with chemical hydrogen-generating system, CAMGCC

The generation of H_2 from the CAMGCC system was identified by using a 6890N network model gas-chromatography system that was connected to a JMS-700 model mass spectrometer. Fig. 2 shows the gas chromatography–mass spectrometry (GC–MS) profiles of gases that were generated from the CAMGCC system by using a gas-over-water technique in degassed distilled H_2O. The product ratio of the generated compounds was determined with high sensitivity from the height and area of the peaks measured using SIM (Selected Ion Monitoring) mode. In Fig. 2, the *x*-axis represents the retention time (min), and the vertical axis represents the intensity. The data show that H_2 was a major product and hydrogen deuteride (HD) was generated from the

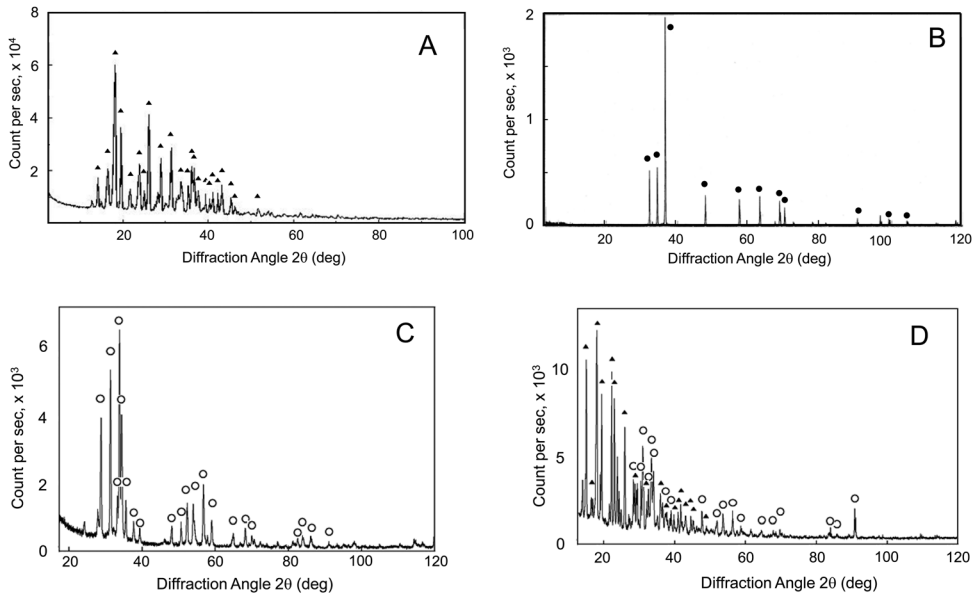

Fig. 1 X-ray powder diffraction (XRD) profiles for citric acid, $CaMg_2$, and CAMGCC systems. The XRD patterns of A, B, C, and D are for citric acid, Mg, $CaMg_2$, and CAMGCC, respectively. $CaMg_2$ (open circles) and citric acid (closed triangles).

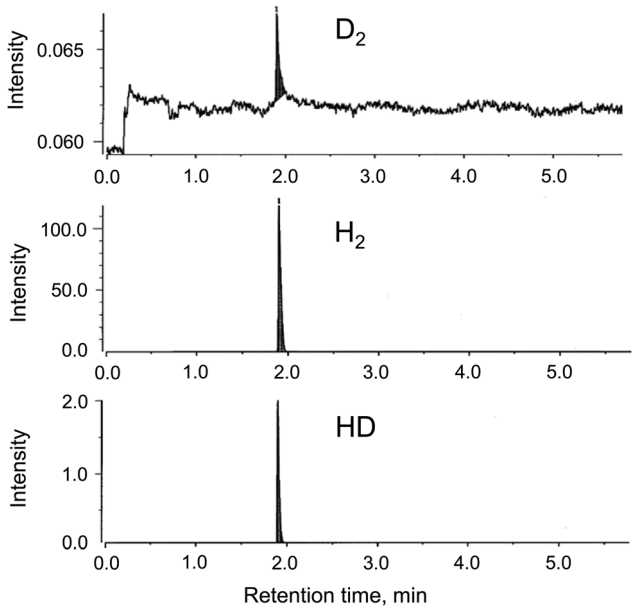

Fig. 2 Identification by gas chromatography–mass spectrometry (GC–MS) analysis of HD, H_2, and D_2 generated from a CAMGCC system in H_2O. GC–MS of gases generated from CAMGCC powders (0.5 g) by the gas-over-water technique. Peak intensity of each compound was measured using SIM mode.

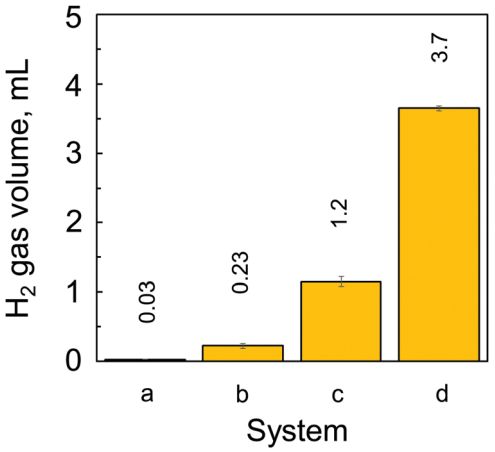

Fig. 3 Measured volume of H_2 generated from Mg (a), $CaMg_2$ (b), MGCC (c), and CAMGCC (d) systems by using the gas-over-water technique. Equimolar (0.27 mmol) amounts of Mg (a), $CaMg_2$ (b), MGCC (c), and CAMGCC (d). Equivalent amounts (0.210 g) of CAMGCC and MGCC. Data are expressed as means ± SEs (standard errors, n = 3).

CAMGCC system at a volume ratio of 1.22% against H_2 because the peak areas of H_2 (m/z 2.0157) and HD (m/z 3.0219) were 219.15 and 2.68, respectively. Gaseous D_2 (m/z 4.02804) was generated simultaneously and the volume ratio was 0.00456%.

Although the reaction between Mg and H_2O occurs as shown by $Mg + 2H_2O \rightarrow Mg^{2+} + 2OH^- + H_2$, H_2 is not generated easily at room temperature in H_2O. To compare the H_2 generation by the CAMGCC system with that of other materials, the volumes of H_2 generated from powder Mg, powder Laves-phase $CaMg_2$, MGCC, and CAMGCC in H_2O were quantified by using the gas-over-water technique. The results are shown in Fig. 3. When 20 mL of H_2O was added to 0.024 g (0.27 mmol) of Laves-phase $CaMg_2$, 0.1 mL of H_2 was generated in 3 min. However, when 20 mL of H_2O was added to 0.21 g (0.27 mmol) of CAMGCC, about 3.8 mL of gaseous H_2 was generated as fine bubbles in 3 min. The CAMGCC equivalent to MGCC generated about 3 times the volume of H_2 by the addition of H_2O as shown in Fig. 3d. The volumes of H_2 generation in the reaction of $CaMg_2$ (in CAMGCC) with H_2O are related to the stoichiometry.

The results show that the volume of H_2 generated in 3 min by an equivalent chemical hydrogen-generating system increases as: Mg < $CaMg_2$ ≪ MGCC < CAMGCC.

Antioxidant activity of chemical hydrogen-generating system, CAMGCC

Hydroxyl radicals. •OH radicals tend to be generated by well-known methods, such as the Fenton system (Fe(II) or Cu(I)/H_2O_2),[16] H_2O radiation,[17] and H_2O_2 photolysis.[13,14] In the photolysis of H_2O_2, 1 mol of H_2O_2 readily forms 2 mol of •OH radicals (eqn (1)).[18] Therefore, we obtained dose–response curves by the scavenging of CAMGCC with •OH from H_2O_2 by irradiation for 60 s at λ 280–315 nm in the dark. The half-maximal (50%) inhibitory concentrations determined from the dose–response curves were used as the antioxidant activity (IC_{50}) of the CAMGCC system.

$$H_2O_2 + UV \rightleftarrows [^{\bullet}OH + {}^{\bullet}OH]_{solvent} \rightarrow 2^{\bullet}OH \quad (1)$$

The hydroxyphenyl fluorescein (HPF) that was oxidized by •OH fluoresces strong signals that absorb an excitation light of λ 490 nm. Importantly, the stock solution of CAMGCC cannot be prepared in advance because CAMGCC generates H_2 in water solution. Therefore, each emission intensity of HPF was measured by adding CAMGCC in a mass range between 0 and 13 mg (in 400 μL) in five-surface transparent quartz cells. Fig. 4A shows the dose–response curves of the HPF responses that were obtained by the scavenging reaction of CAMGCC with •OH. The x-axis shows the concentration of CAMGCC and the y-axis shows the relative fluorescence intensity (F). The IC_{50} represents the 50% fluorescence intensity point of the dose–response curve of the F response for various concentrations of CAMGCC. The antioxidant activities of MGCC and Trolox (6-hydroxy-2,5,7,8-tetramethylchroman-2-carboxylic acid) were compared with those of CAMGCC under similar conditions because Trolox has been used as an antioxidant standard.[19] The results are shown in Fig. 4B and C. The •OH scavenging activities of CAMGCC, MGCC, and Trolox were 4.2 (±0.262), 5.0 (±0.225) (±SE), and 1.25 × 10^{-4} mg mL^{-1}, respectively. The values of IC_{50} (means) are summarized in Fig. 4D. The small bars represent standard errors (SE). The strength of the antioxidant activity increased as: MGCC < CAMGCC ≪ Trolox. Excess •OH that was generated by H_2O_2 photolysis is scavenged by H_2 that is generated from CAMGCC in H_2O (Fig. 4E). The reaction mechanism is given by the reaction $H_2 + 2^{\bullet}OH \rightarrow 2H_2O$.

Superoxide anion radicals. The scavenging activity of the superoxide anion radical ($O_2^{-\bullet}$) was determined from the change in chemiluminescence (F_{CL}) response by the reaction of MPEC

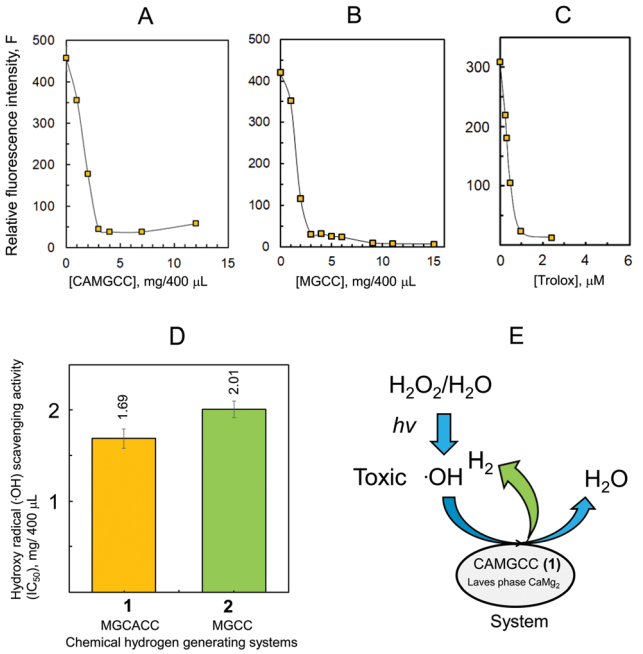

Fig. 4 Dose–response curves of CAMGCC (A) and MGCC (B) for hydroxyl-radical (•OH) scavenging activity and the IC_{50} diagram (D). Responses are expressed as the intensity of fluorescence for the concentration (mg/400 μL) of CAMGCC (A), MGCC (B), and Trolox (C) in 10 mM phosphate buffer (pH 7.4). (D) IC_{50} values are converted to values for 1 mL. Data are expressed as means ± SEs (n = 3). (E) Model of scavenging reaction by the reaction of toxic •OH formed by photolysis with H_2 generated from CAMGCC in H_2O.

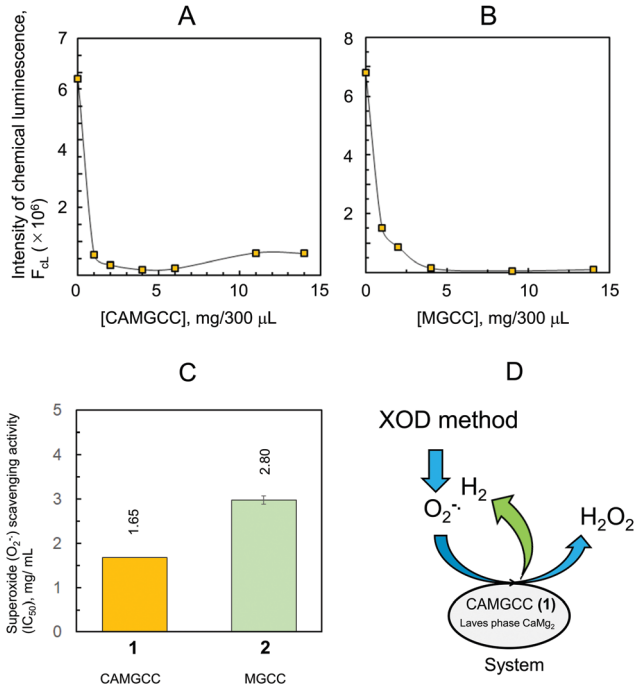

Fig. 5 Dose–response curves for superoxide anion-radical ($O_2^{-\bullet}$) scavenging of CAMGCC (A) and MGCC (B) and the IC_{50} diagram (C). Responses are expressed as the intensity of chemiluminescence for the concentration (mg/300 μL) of CAMGCC and MGCC in 10 mM phosphate buffer (pH 7.4). MPEC is used as a chemiluminescent reagent. Data are expressed as means ± SEs (n = 4). (D) Model of ROS scavenging by the reaction of $O_2^{-\bullet}$ (formed by XOD/HPX method) with H_2 (generated from CAMGCC in 0.1 M phosphate buffer).

with the $O_2^{-\bullet}$ produced by the XOD-HPX method.[20] In the $O_2^{-\bullet}$ scavenging reaction, the control value (F_{CL}) was 5–7 × 10^6 (RLU). Fig. 5 shows the dose–response curves for $O_2^{-\bullet}$ scavenging measured at 6–7 points of a mass range between 0 and 14 mg (in 400 μL) of CAMGCC (A) and MGCC (B). In the series of measurements, the $O_2^{-\bullet}$ scavenging activities of CAMGCC and MGCC were 1.68 (±0.089) and 2.97 (±0.88) (±SE) mg mL^{-1}, respectively. The results are summarized in Fig. 5C. In comparison with CAMGCC, Trolox was 0.0166 (±0.00375) mg mL^{-1} (= 6.63 × 10^{-5} ± 1.5 × 10^{-5} (±SE) mol L^{-1}). The antioxidant activity strength increased as: MGCC < CAMGCC < Trolox. When using Mg_3(citric acid)$_2$ instead of CAMGCC, the $O_2^{-\bullet}$ scavenging reaction did not proceed. Therefore, we propose that the active species in the CAMGCC system is H_2 that is generated from CAMGCC in H_2O (Fig. 5D).

Crystal structure of Laves-phase $CaMg_2$ and structural model of the $CaMg_2$ cluster

The experimental lattice parameters and space groups of the Laves-phase $CaMg_2$ (**3**) and Mg (**4**) that were used to prepare the CAMGCC and MGCC systems were taken from the literature,[21–23] and the $CaMg_2$ and Mg structures were prepared by using VESTA and Spartan'16 as shown in Fig. 6. Fig. 7A and B show the energy levels and the highest occupied molecular orbital (HOMO) and lowest unoccupied molecular orbital (LUMO) phases of Laves-phase **3** calculated using the B3LYP method with 6-311+G(2df,2p) as the basis set. The energy, ε_{homo}, ε_{lumo}, absolute hardness (η), and absolute electronegativity (χ) of **3** and **4** are listed in Table 1. The ε_{homo} (−3.37 eV) of Laves-phase **3** is higher than that (−3.41 eV) of crystal Mg **4**. Crystal **3** from eqn (5) is a harder crystal chemically than crystal **4**, and the absolute electronegativity (χ = 3.020) of **3** is lower than that (χ = 3.170) of **4**. That is, the Laves phase of **3** is more easily oxidized than crystal **4**. Fig. 7C shows the energy levels and the HOMO and LUMO phases of crystal Mg **4** that were computed by using the B3LYP/and M06/6-311+G(2df,2p) methods. The HOMO and LUMO phases of $CaMg_2$ **3** are distributed on the Ca and two Mg atoms that are represented by ▲ in the crystal. The HOMO phase of Mg **4** is distributed on the three Mg atoms represented by ▲ in the crystal. The HOMO phase of Laves-phase **3** is distributed in the Ca of ▲ as shown in Fig. 6 and 7A and B.

We present the cluster of $CaMg_2$ (**5**) and Mg_3 (**6**) shown as ▲ in crystals **3** and **4** in Fig. 6. Fig. 7D shows the optimized structures, the HOMO and LUMO phases, and energy levels of clusters **5** and **6**. The calculated data are listed in Table 2. The results show that **6** has two energetically stable structures, **6a** and **6b**. The difference of the energies of **6a** and **6b** calculated by B3LYP/6-311+G(2df,2p) is small; the energies are −16334.72 (**6a**) and −16334.58 eV (**6b**). The bond lengths, Mg–Mg, of **6a** and **6b** are 3.44 and 6.74 Å, respectively. The binding energy of **5** is 0.216 eV, a value that is obtained by subtracting the basis set superposition error (BSSE[24]). The HOMO is distributed in the Ca of the $CaMg_2$ cluster **5** (Fig. 7B). From Table 2, the absolute electronegativity of the $CaMg_2$ cluster **5** is lower than that of Mg

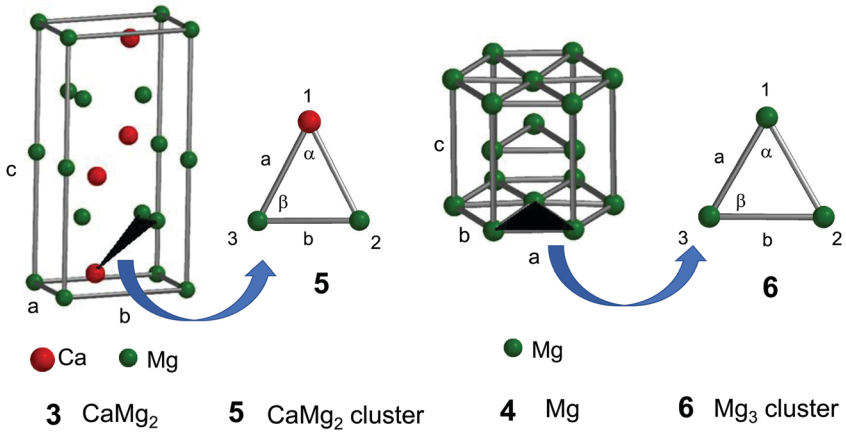

Fig. 6 Crystal structures of Laves-phase $CaMg_2$ (**3**) and Mg (**4**) and structural models of the $CaMg_2$ cluster (**5**) and Mg_3 cluster (**6**). For a detailed description of **3** and **4**, see Fig. 7A and B. Models of clusters **5** and **6** are represented by ▲ in the structures of **3** and **4**.

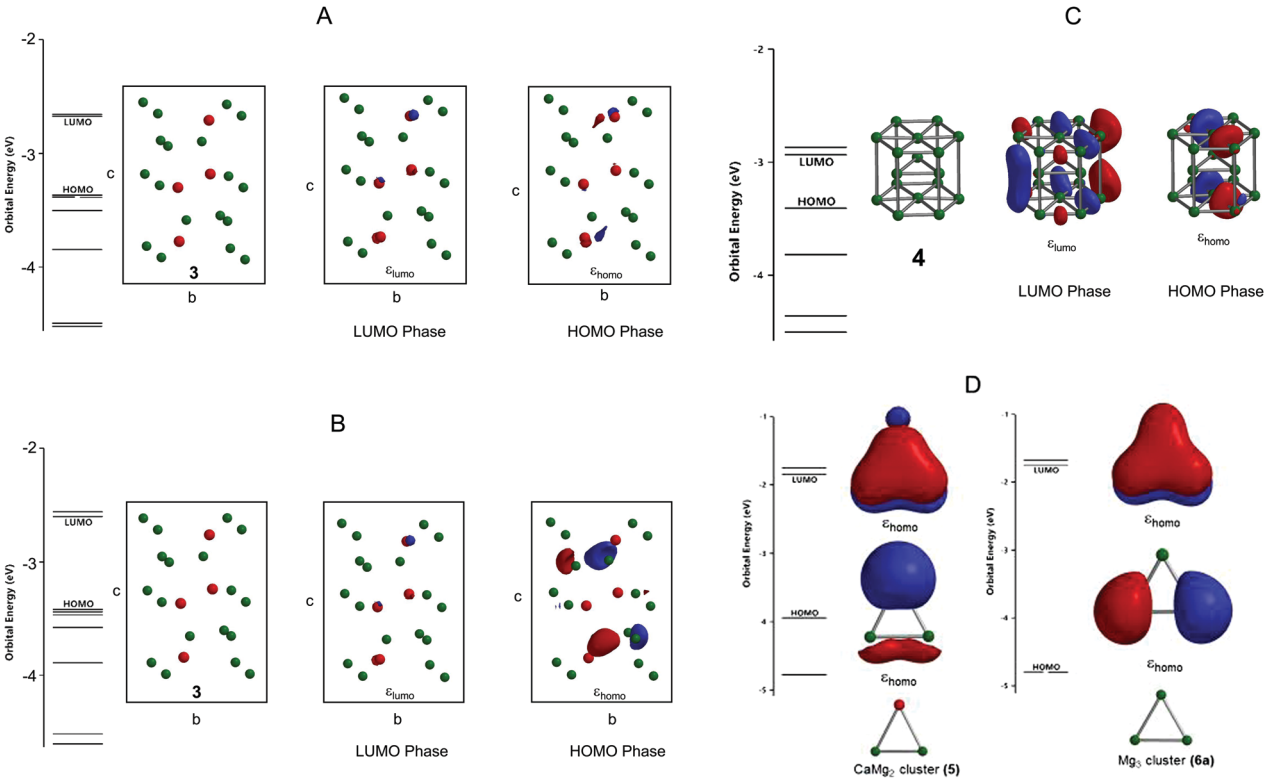

Fig. 7 Orbital energy diagram and the HOMO and LUMO phases of Laves-phase $CaMg_2$ (A and B), crystal Mg (C), $CaMg_2$, and Mg_3 clusters (D). (A and B) Single-point orbital energy, ε_{homo}, and ε_{lumo} of $CaMg_2$ computed at the B3LYP/6-311+G(2df,2p) and M06/6-311+G(2df,2p) level, respectively. The structural parameters of $CaMg_2$ are $a = b = 6.220$ Å, $c = 10.100$ Å, $\alpha = \beta = 90°$, and $\gamma = 120°$. (C) Orbital energy, ε_{homo}, and ε_{lumo} of crystal Mg computed at the B3LYP/6-311+G(2df,2p) level. (D) Orbital energy, ε_{homo}, and ε_{lumo} for clusters of $CaMg_2$ and Mg_3 optimized using the B3LYP/6-311+G(2df,2p) method.

cluster **6a**; the electron-withdrawing property of the Mg cluster **6a** is stronger than that of the $CaMg_2$ cluster **5**. Furthermore, cluster **5** (η = 1.060) with a small HOMO–LUMO gap has a higher reactivity than **6a** (η = 1.515) with a large hardness.

Electron transfer to H_2O from $CaMg_2$ and Mg

The CAMGCC scavenges •OH radicals, and we found that the antioxidant activity of CAMGCC is stronger than that of MGCC as shown in Fig. 4 and 5. We explored why the antioxidant activity of CAMGCC is stronger than that of MGCC. The difference in reactivity of $CaMg_2$ **3** and Mg **4** is derived from the quantity of electron transfer (ΔQ) based on chemical hardness as shown in eqn (6), because H_2 generation by the reaction of CAMGCC with H_2O is a redox reaction. Tables 1 and 2 show the values of the absolute hardness (η) and absolute electronegativity (χ) of the crystal models **3** and **4**.

An electron is transferred from Laves-phase $CaMg_2$ **3** to H_2O because the ΔQ value is negative (−0.11) according to the approximation of eqn (6). Similarly, the ΔQ of crystal Mg **4** is

Table 1 Energy, ε_{homo}, ε_{lumo}, absolute hardness and electronegativity of Laves phase $CaMg_2$ and Mg computed using the DFT method

	Distance[a]							
	a (Å)	b (Å)	c (Å)	Energy[b] (eV)	ε_{homo} (eV)	ε_{lumo} (eV)	Absolute hardness (η, eV)	Absolute electronegativity (χ, eV)
$CaMg_2$ (**3**)	6.220	6.220	10.100					
B3LYP/6-311+G(2df,2p)				−171764.59	−3.37	−2.67	0.3505	3.020
6-311+G(d,p)				−171764.22	−3.38	−2.69	0.345	3.035
M06/6-311+G(2df,2p)				−171747.93	−3.42	−2.60	0.410	3.010
Mg (**4**)	3.209	3.209	5.211					
B3LYP/6-311+G(2df,2p)				−92550.01	−3.41	−2.93	0.240	3.170
6-311+G(d,p)				−92549.63	−3.44	−2.74	0.233	3.090
M06/6-311+G(2df,2p)				−92541.90	−3.51	−2.67	0.420	3.090
H_2O								
6-311+G(2df,2p)				−2080.67[c]	−8.82	0.56	4.69	4.13

[a] a, b, and c present crystal parameters. [b] Single-point calculation. [c] Optimized energy.

Table 2 Energy, ε_{homo}, ε_{lumo}, absolute hardness and electronegativity of $CaMg_2$ and Mg_3 clusters computed using the DFT method

	Distance		Bond angle						
	a (Å)	b (Å)	(α) (degree)	(β) (degree)	Energy[a] (eV)	ε_{homo} (eV)	ε_{lumo} (eV)	Absolute hardness (η, eV)	Absolute electronegativity (χ, eV)
$CaMg_2$ cluster (**5**)									
B3LYP/6-311+G(2df,2p)	3.667	3.349	54.3	62.8	−29327.93	−3.96	−1.84	1.060	2.900
M06/6-311+G(2df,2p)	3.510	3.201	54.2	62.9	−29325.14	−4.02	−1.79	1.115	2.905
Mg_3 cluster (**6a**)									
B3LYP/6-311+G(2df,2p)	3.44	3.44	60.0	60.0	−16334.72	−4.79	−1.76	1.515	3.280
M06/6-311+G(2df,2p)	3.237	3.237	60.0	60.0	−16332.15	−4.76	−1.74	1.510	3.250
Mg_3 cluster (**6b**)									
B3LYP/6-311+G(2df,2p)	6.74	6.74	60.0	60.0	−16334.58	−5.26	−1.17	2.045	3.215

[a] Optimized energy.

−0.097. The magnitude of ΔQ is greater for **3** than for **4**. The results suggest that the reductive power of **3** is stronger than **4**. The difference in ΔQ values of **3** > **4** for electron transfer also suggests that the antioxidant activity of the CAMGCC system is stronger than that of the MGCC system. The ΔQ of the electrons from crystals **3** (and **4**) to H_2O is equivalent to systems **1** (and **2**). To test the above results, the ΔQ of the electrons from clusters **5** and **6a** to H_2O were calculated and the results are listed in Table 3. The magnitude of ΔQ is in the following order: **5** ($\Delta Q = -0.107$) > **6a** ($\Delta Q = -0.069$) at the B3LYP/6-311+G(2df,2p) level. Part of the reason that the chemical hydrogen-generating system CAMGCC was prepared by using Laves-phase $CaMg_2$ as a superior antioxidant to MGCC prepared by using crystal Mg is related to its chemical hardness (Fig. 8).

We report for the first time the chemical properties, reactivity, and antioxidant activity of a new chemical hydrogen-generating system, CAMGCC, prepared using Laves-phase $CaMg_2$. The CAMGCC generated gaseous H_2 by the effect of solid citric acid on the CAMGCC's surface in water, and showed the selective scavenging activity of $^{\bullet}OH$ generated by the ultraviolet (UV) photolysis of H_2O_2. $CaMg_2$ is classified as Laves-phase AB_2, and is well known for its chemical storage of H_2. Zirconium-based and $NiMg_2$ alloys have been developed for the reversible storage of H_2.[25,26] However, the CAMGCC system reported in this study was not prepared for use as a prospective hydrogen-storage material but rather for use as a hydrogen-generating system that can generate H_2 rapidly in water. CAMGCC has different chemical properties for the oxidation-resistance of $CaMg_2$ alloys because the CAMGCC by the effect of the citric acid on the $CaMg_2$ surface is oxidized easily in H_2O. The amount of H_2 that is generated from the CAMGCC system was 4 ml (0.27 mmol of $CaMg_2$) for 3 min, which is about 3 times the amount of H_2 produced from an equimolar amount (0.27 mmol of Mg) of MGCC (eqn (2)). Therefore, the stoichiometry of the reaction of $CaMg_2$ (CAMGCC) with H_2O is best expressed by eqn (3).

$$Mg\ (MGCC) + 2H_2O \rightarrow Mg(OH)_2 + H_2 \quad (2)$$

$$CaMg_2\ (CAMGCC) + 6H_2O \rightarrow Ca(OH)_2 + 2Mg(OH)_2 + 3H_2 \quad (3)$$

Although the gaseous H_2, D_2, and HD that were generated from CAMGCC in H_2O were identified by using a GC–MS technique (Fig. 2), the bands of D_2 and HD were derived from D_2O, including in water. The equilibrium constant (K) of H_2O and D_2O is 4, and it is expressed in the following equilibrium, $H_2O + D_2O \rightleftarrows 2HDO$ ($K = 4$).[27] Therefore, HD observed by GC–MS measurements was produced by the reaction of CAMGCC with HDO.

Table 3 Calculated quantity of electron transfer (ΔQ) from $CaMg_2$ and Mg to H_2O by redox reaction

System	Method	Metal	Medium	Quantity of electron transfer (ΔQ)
CAMGCC				
	B3LYP/6-311+G(2df,2p)	$CaMg_2$ (**3**)	H_2O	−0.11
	M06/6-311+G(2df,2p)	**3**	H_2O	−0.11
	B3LYP/6-311+G(2df,2p)	$CaMg_2$ cluster (**5**)	H_2O	−0.107
	M06/6-311+G(2df,2p)	**5**	H_2O	−0.107
MGCC				
	B3LYP/6-311+G(2df,2p)	Mg (**4**)	H_2O	−0.097
	M06/6-311+G(2df,2p)	**4**	H_2O	−0.096
	B3LYP/6-311+G(2df,2p)	Mg_3 cluster (**6a**)	H_2O	−0.069
	M06/6-311+G(2df,2p)	**6a**	H_2O	−0.074

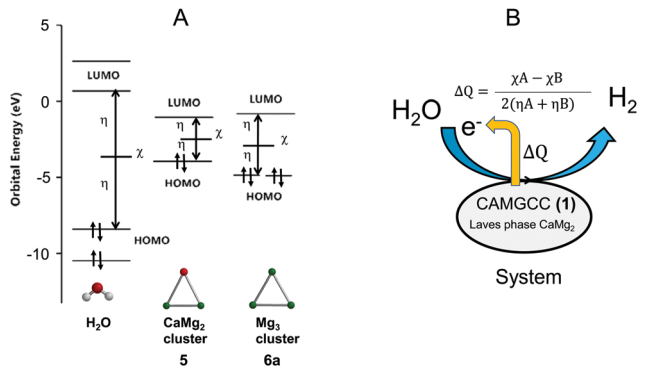

Fig. 8 Orbital energy diagram, HOMO, and LUMO phases for optimized models of $CaMg_2$ and Mg clusters, and hardness (η) and electronegativity (χ) of H_2O, $CaMg_2$, and Mg_3 clusters (A) and H_2 generation by the reaction of CAMGCC with H_2O (B). (A) The orbital energy, ε_{homo}, and ε_{lumo} for clusters of $CaMg_2$ and Mg_3 optimized by using the B3LYP/6-311+G(2df,2p) method. The η and χ are shown in the diagram of the H_2O, $CaMg_2$, and Mg_3 clusters. The values of 2η and χ are equal to $I_p - E_a \fallingdotseq \varepsilon_{homo} - \varepsilon_{lumo}$ and $I_p - \eta \fallingdotseq \varepsilon_{homo} - \eta$, respectively. (B) Model of H_2 generation by the reaction of CAMGCC with H_2O on the CAMGCC surface.

The CAMGCC system proved a useful antioxidant to scavenge reactive oxygen species, such as $O_2^{-\bullet}$ and $^\bullet$OH. The scavenging of toxic $^\bullet$OH translates biologically into a reduction of the oxidative stress of cells, living tissues, and body systems. We explored the antioxidant activity of CAMGCC by the reaction of CAMGCC with $^\bullet$OH generated from the photolysis of H_2O_2 as a biological model of $^\bullet$OH. Hydrogen gas was generated vigorously with fine bubbles in the five-surface transparent quartz cell to which CAMGCC was added. Fine H_2 bubbles that were generated from the CAMGCC surface scavenged the $^\bullet$OH generated by the UV photolysis of H_2O_2. The CAMGCC system prepared with Laves-phase $CaMg_2$ has a stronger $^\bullet$OH scavenging activity than the MGCC prepared with Mg as shown in Fig. 4. The $^\bullet$OH scavenging activity (IC_{50}) of CAMGCC was 1.68 ± 0.105 (mg/400 μL), and the IC_{50} converted to moles is equal to 5.96 mM. The IC_{50} is for a molecular weight of $CaMg_2$ (M.W. = 88). The IC_{50} of Trolox is usually used as a standard for scavenging activity. The scavenging activity of CAMGCC was 1/50 times that of Trolox, as shown in Fig. 4. Although CAMGCC is not as strong an antioxidant as Trolox and other polyphenols, it is thought that the new system, CAMGCC, is an antioxidant that scavenges highly toxic $^\bullet$OH selectively.

The CAMGCC and MGCC were prepared using Laves-phase $CaMg_2$ and Mg, respectively, and the lattice structures of $CaMg_2$ and Mg were classified as hexagonal *P*63/*mmc* (No. 194) (Fig. 6). Clusters **5** and **6** are considered to be cluster approximations of **3** and **4** because the η and χ of clusters **5** and **6** have a trend that is similar to that of crystals $CaMg_2$ **3** and Mg **4**. The calculated 0.216 eV for the binding energy of Ca–Mg of **5** was smaller than the 46.4 kcal mol^{-1} of cluster Cu–Cu.[28] That is, $CaMg_2$ is known to be a brittle alloy. We showed that the chemical hardness of clusters $CaMg_2$ and Mg plays a key role in understanding the mechanism of the antioxidant reaction of CAMGCC **1** and MGCC **2**. The ΔQ values of electron transfer between CAMGCC (and MGCC) and H_2O are an important quantity for understanding why the $^\bullet$OH scavenging activity of CAMGCC is stronger than that of MGCC; namely, the $^\bullet$OH scavenging activity by CAMGCC results from a redox reaction of CAMGCC with H_2O. To develop an effective hydrogen-generating system, we have to consider that Laves-phase AB_2 structures possess a small absolute hardness and a large absolute electronegativity. The theoretical results in Table 3 suggest that the ΔQ of electron transfer from Laves-phases AB_2 to H_2O can be used to develop $^\bullet$OH and $O_2^{-\bullet}$ scavenging active chemical hydrogen-generating systems. Therefore, the absolute hardness and ΔQ values are useful parameters for developing a chemical hydrogen-generating system with a strong reducing power. It can be predicted that the ΔQ values of electron transfer from metals and alloys to water are a determining factor in the development of an excellent chemical hydrogen-generating system as shown in Fig. 8B.

Conclusions

We developed a new chemical hydrogen-generating system CAMGCC using a Laves-phase $CaMg_2$ alloy prepared by arc melting. The CAMGCC generated H_2 readily by H_2O addition. Our study revealed for the first time that Laves-phase $CaMg_2$ is superior to Mg to prepare a chemical hydrogen-generating system, because the equimolar H_2 gas volume quantified by using the gas-over-water technique was higher in $CaMg_2$ than in Mg (Fig. 3). Our results show that the CAMGCC is an excellent antioxidant (Fig. 4D and 5C). The CAMGCC scavenged highly toxic $^\bullet$OH and $O_2^{-\bullet}$ selectively, which are well known to be the cause of many diseases in the living body. Therefore, the development of antioxidant materials that scavenge ROS is important for materials science and from the viewpoint of medical care. We propose that the ΔQ of electron transfer from Laves-phase AB_2 to H_2O is an important parameter to develop chemical hydrogen-generating systems. The results were supported by the calculated ΔQ of electron transfer by the reaction of the crystal structures of the Laves-phase $CaMg_2$ and Mg calculated by a DFT method, B3LYP/6-311+G(2df,2p) and M06/6-311+G(2df,2p), with H_2O. As a clarification of the results, our datashow that $CaMg_2$ (−0.107, Table 3) has a larger ΔQ of charge

transfer to H_2O than Mg_3 (−0.069, Table 3) as demonstrated by the cluster model. Applications of a material CAMGCC system containing Ca to the prevention of disease by oxidative stress can be expected in the future.

Materials and methods

Materials

Magnesium metal powder, calcium metal shot, and citric acid (anhydride) were obtained from Wako Pure Chemical Industries, Ltd (Osaka, Japan). Mg_3(citric acid)$_2$ was obtained from Tokyo Chemical Industry Co. Ltd (Tokyo, Japan). Hydroxyphenyl fluorescein (HPF) was obtained from Sekisui Medical Co. Ltd (Tokyo, Japan). The MGCC system was obtained from Nikko-Kasei Co. Ltd (Tokyo, Japan). Standard hydrogen (H_2, 99.99% purity) was obtained from GL Sciences Inc. (Tokyo, Japan). Xanthinoxidase (10 U) and hypoxanthine were obtained from Calbiochem (Darmstadt, Germany). All experimental solutions were prepared with degassed distilled water (DW). All other chemicals used were of the highest grade available.

Procedure of the $CaMg_2$ Laves phase and chemical hydrogen-generating (CAMGCC) system

3.4468 g (0.0860 mol) of sheet Ca and 4.0104 g (0.1717 mol) of metal Mg were arc melted together and the Ca–Mg alloy was homogenized under high-purity argon (Ar) gas after evacuation to 3 Pa in a compact arc melting furnace (Diavac Ltd, Chiba, Japan). Air in the glove box was exchanged in Ar flow (7.0 L min^{-1} for 60 min, 500 L). The box was turned nine times to homogenize the Ca–Mg alloy during arc melting. After arc melting, the Ca–Mg alloy was converted to a fine powder by crushing with a pestle in a porcelain mortar (MP-90, Niigata Seiki Co. Ltd, Sanjo, Japan).

Powder X-ray diffraction method

Powder X-ray diffraction (XRD) measurements were taken on an Ultima IV diffractometer (Rigaku, Tokyo, Japan) using CuKα radiation. The X-ray tube voltage and current were 40 kV and 40 mA, respectively. Data were collected at 2θ from 3° to 120° angle ranges. The detection interval was at a 2θ step of 0.02°.

Chemical hydrogen-generating (CAMGCC) system procedure

The $CaMg_2$-hydroxypropyl cellulose (HPC)–citric acid (CAMGCC) system was prepared by the physical mixing of 1.0 g of $CaMg_2$–HPC (prepared by the physical mixing of 1.0 g of Laves-phase $CaMg_2$ with 0.072 g of HPC) with 7.2 g of citric acid (anhydrous).

Gas chromatography–mass spectrometry

The mass spectra of H_2, HD, and D_2 gases were collected using a model 6890N network gas chromatography system (Agilent Technologies, Japan) connected to a Model JMS-700 mass spectrometer (JEOL Ltd, Tokyo, Japan).[10] The insoluble gases H_2, D_2, and HD produced from the CAMGCC system in H_2O, respectively, were collected and identified by using gas-over-water and injected directly into a helium carrier gas by using a gas-tight instrument syringe (1 mL, Model 1001 RN SYR, Hamilton Co.). The peaks were measured by a rate of temperature increase from 30 to 120 °C. The hydrogen gas peak by GC–MS was identified by using standard hydrogen. RT®-Msieve 5A columns (30 m × 0.32 mm, coated with 30-μm thick molecular sieves) (RESTEK Co., Bellefonte PA, USA) were used for the helium carrier gas. Gas chromatography was used to introduce the generated gases into the mass spectrometer. The injector and detector temperatures were maintained at 30 °C. EI mass spectra were acquired over a mass range of m/z 0 to 40. The ratio of generated D_2, H_2, and HD ions (m/z) was obtained from the height or area value of each peak of the GC spectrum using the SIM mode.

Crystal structure and chemical hardness of Laves-phase $CaMg_2$

The crystal structures of Laves-phase $CaMg_2$ and Mg comprise a hexagonal close-packed (hcp) system with a space group $P63/mmc$ (No. 194). The experimental parameters of Laves-phase $CaMg_2$ (**3**)[21,22] and Mg (**4**)[23] are $a = b = 6.220$ Å, $c = 10.100$ Å, $\alpha = \beta = 90°$, and $\gamma = 120°$ and $a = b = 3.209$ Å, $c = 5.2105$ Å (see Fig. 6), respectively. The crystal structures of $CaMg_2$ and Mg were visualized using VESTA (three-dimensional visualization system of crystal structures) and modeled using Spartan'16 (Wavefunction, Inc., Irvine, CA, U.S.A.). The electron energy, the HOMO and LUMO (frontier orbitals) energy levels, and the orbital phases of crystals $CaMg_2$ **3** and Mg **4** were single-point computed using B3LYP and M06 methods by DFT with 6-311+G(2df,2p) and 6-311+G(d,p) as the basis set. To understand the electronic states of crystal $CaMg_2$ and Mg, optimized structures of clusters of $CaMg_2$ (**5**) and Mg_3 (**6**) were computed using B3LYP and M06 methods with 6-311+G(2df,2p) as the basis set. The calculated values were collected using Spartan'16. The binding energies of Ca–Mg and Mg–Mg in the $CaMg_2$ and Mg_3 clusters were corrected for BSSE by using the counterpoise (CP) correction. For each calculation, the BSSE-corrected value was obtained using the keyword "INTERACTIONENERGY = BSSE".

The absolute hardness (η) and absolute electronegativity (χ) were calculated from eqn (4) and (5) as defined by Parr and Pearson:[29,30]

$$\chi = -\mu = -(\partial E/\partial N)_{v(r)} = (I_p + E_a)/2 = -(\varepsilon_{LUMO} + \varepsilon_{HOMO})/2 \quad (4)$$

$$\eta = (\partial \mu/\partial N)_{v(r)}/2 = (\partial^2 E/\partial N^2)/2 = (\varepsilon_{LUMO} - \varepsilon_{HOMO})/2 \quad (5)$$

where E is the electronic energy of a molecule, N is the number of electrons, $v(r)$ is the external electrostatic potential, and I_p and E_a are the ionization energy and the electron affinity (eV). According to Koopmans' theorem, the ε_{HOMO} and ε_{LUMO}, which are the energy levels for the frontier orbitals, are roughly equal to I_p and E_a, respectively.

The quantity of electron transfer (ΔQ) has been given by eqn (6):[29,31]

$$\Delta Q = (\chi A - \chi B)/2(\eta A + \eta B) \quad (6)$$

If ΔQ is positive, the electrons are transferred from A to B. If ΔQ is negative, the electrons are transferred from B to A. The reaction between CAMGCC (and MGCC) (A) and H_2O (B) is a redox reaction because the CAMGCC (and MGCC) system is oxidized by H_2O.

Generation of hydroxyl radicals (OH•) by UV photolysis

Hydroxy radicals (•OH) were generated by ultraviolet (UV) photolysis. The generated •OH radicals were detected using hydroxyphenyl fluorescein (HPF)[32] as a fluorescent probe, which becomes strongly fluorescent by reaction with •OH. HPF (100 μL, 5 μM) in 10 mM phosphate solution (pH 7.4) was added to a five-surface transparent quartz cell (10 mm × 10 mm × 45 mm) that contained 300 μL of 3% H_2O_2 in 10 mM phosphate (pH 7.4). The solution was irradiated by UV for 60 s using the UV transilluminator (λ = 315 nm, TP-20ME, ATTO Co., Japan) in the dark. After UV irradiation, a total volume of 3 mL solution was prepared to measure its relative fluorescence intensity (F) by adding 10 mM phosphate buffer (pH 7.4) to the quartz cell and by collecting the F values by spectrofluorophotometer (JASCO FP-6200, JASCO Co., Tokyo, Japan). Wavelengths of 490 and 515 nm were used as excitation and emission wavelengths, respectively.

Scavenging of hydroxyl radicals (•OH) by the CAMGCC system

The •OH scavenging reaction was performed by adding 0, 1, 2, 3, 4, 5, 8, 11, and 15 mg each of CAMGCC to 400 μL of the quartz cell solution described above. After mixing by mild pipetting two times and UV irradiation for 60 s, 10 mM phosphate buffer (pH 7.4) was added to prepare a final volume of 3 mL of the UV irradiated solution mix. Wavelengths of 490 and 515 nm were used as excitation and emission wavelengths, respectively.

Scavenging of superoxide anion radicals ($O_2^{-\bullet}$) by the CAMGCC system

Superoxide anion radicals ($O_2^{-\bullet}$) were generated by using the xanthine oxidase-hypoxanthine (XOD-HPX) system and $O_2^{-\bullet}$ was emitted to reduce 2-methyl-6-*p*-methoxyphenylethynyl-imidazopyrazinone (MPEC) (ATTO Co., Tokyo, Japan), which yielded a chemiluminescent product. The chemiluminescence intensity (F_{CL}) was measured with a lumicounter (Lumat LB9507, Berthold). The XOD (0.1 U mL^{-1}) and HPX (1.5 mM prepared from 7.5 mM HPX) were prepared with 0.1 M phosphate buffer (pH 7.5). The $O_2^{-\bullet}$ scavenging reaction was performed in 300 μL at 25 °C by mixing XOD (60 μL), 0.1 M phosphate buffer (160 μL), and MPEC (10 μL in DW). Test compounds were mixed in test tubes (20 μL) immediately before HPX addition (50 μL), and the final concentrations of the test systems, CAMGCC (**1**) and MGCC (**2**), were 0, 1, 2, 4, 6, 9, 11, and 14 mg. The reaction mixtures were incubated at 37 °C in a water bath for 10 s. The reaction solution without the test systems was equilibrated to the desired level of F_{CL} output for 1 min. The half-maximal inhibitory concentration (IC_{50}) was calculated from the dose–F_{CL} curve obtained from measured F_{CL}, and the concentrations of the test systems were as shown in Fig. 5A–C.

Conflicts of interest

There are no conflicts to declare.

Acknowledgements

The authors would like to thank Dr Masahiro Uda for helpful discussions and for the arc melting techniques.

References

1 A. F. Dale brook, W. Gan, M. Grasermann, S. Moret and G. Laurenczy, *Chem. Commun.*, 2013, **49**, 8735–8751.
2 Y. H. Hu, *Int. J. Energy Res.*, 2013, **37**, 683–685.
3 I. Ohsawa, M. Ishikawa, K. Takahashi, M. Watanabe, K. Nishimaki, K. Yamagata, K. Katsura, Y. Katayama, S. Asoh and S. Ohta, *Nat. Med.*, 2007, **13**, 688–694.
4 K. Ohno, M. Ito, M. Ichihara and M. Ito, *Oxid. Med. Cell. Longevity*, 2012, 11.
5 S. Ohta, *Pharmacol. Ther.*, 2014, **144**, 1–11.
6 J. F. Fan, C. L. Yang, G. Han, S. Fang, W. D. Yang and B. S. Xu, *J. Alloys Compd.*, 2011, **509**, 2137–2142.
7 J. F. Stampfer, C. E. Holley Jr and J. F. Scttle, *J. Am. Chem. Soc.*, 1960, **82**, 3504–3508.
8 N. Terashita and E. Akiba, *Mater. Trans.*, 2004, **45**, 2594–2597.
9 T. Nobuki, M. Chiba and T. Kuji, *J. Alloys Compd.*, 2007, **446**, 152–156.
10 S. Kobayashi, T. Chikuma, K. Chiba, D. Tsuchiya and T. Hirai, *J. Mol. Struct.*, 2016, **1106**, 468–478.
11 O. Shimomura, C. Wu, A. Murai and H. Nakamura, *Anal. Biochem.*, 1998, **258**, 230–235.
12 P. Attri, Y. H. Kim, D. H. Park, J. H. Park, Y. J. Hong, H. S. Uhm and K.-N. Kim, *Nat. Sci. Rep.*, 2015, **5**, 9332–9339.
13 O. Legrini, E. Oliveros and A. M. Braun, *Chem. Rev.*, 1993, **93**, 671–698.
14 S. Gligorovski, R. Strekowski, S. Barbati and D. Vione, *Chem. Rev.*, 2015, **115**, 13051–13092.
15 J. Jellinek and P. H. Acioli, *J. Phys. Chem. A*, 2002, **106**(45), 10919–10925.
16 C. Walling, *Acc. Chem. Res.*, 1975, **8**, 125–131.
17 L. M. Kohan, S. Sanguanmith, J. Meesungnoen, P. Causey, C. R. Stuart and J.-P. Jay-Gerin, *RSC Adv.*, 2013, **3**, 19282–19299.
18 H. Herrmann, *Phys. Chem. Chem. Phys.*, 2007, **9**, 3935–3964.
19 R. Re, N. Pellegrini, A. Proteggente, A. Pannala, M. Yang and C. Rice-Evans, *Free Radical Biol. Med.*, 1999, **26**, 1231–1237.
20 S. Kobayashi and S. Kanai, *Molecules*, 2013, **18**, 6128–6141.
21 K. Aono, S. Orimo and H. Fujii, *J. Alloys Compd.*, 2000, **309**, L1–L4.
22 J. Fu, W. Lin and Z. Chen, *Int. J. Advanced Materials and Production*, 2016, **1**, 62–69.
23 M. D. Graef and M. McHerry, *Crystal Structure Descriptions*, 2nd edn, 2013, http://som.web.cmu.edu/frames2.html.
24 S. F. Boys and F. Bernardi, *Mol. Phys.*, 1970, **19**, 553–566.
25 D. G. Ivey and D. O. Northwood, *Z. Phys. Chem.*, 1986, **147**, 191–209.
26 S. B. Gesari, M. E. Pronsato, A. Visintin and A. Juan, *J. Phys. Chem. C*, 2010, **114**, 16832–16836.
27 L. Friedman and V. J. Shiner Jr., *J. Chem. Phys.*, 1966, **44**, 4639–4640.
28 M. D. Morse, *Chem. Rev.*, 1986, **86**, 1049–1109.
29 R. G. Parr and R. G. Pearson, *J. Am. Chem. Soc.*, 1983, **105**, 7512–7516.
30 R. G. Pearson, *J. Chem. Sci.*, 2005, **117**(5), 369–377.
31 W. Kohn, A. D. Becke and R. G. Parr, *J. Phys. Chem.*, 1996, **100**, 12974–12980.
32 K. Setukinai, Y. Urano, K. Kakinuma, H. J. Majima and T. Nagano, *J. Bio. Chem.*, 2003, **278**, 3170–3175.

